

Electrochemical Fluorescence Switching Properties of Conjugated Polymers Composed of Triphenylamine, Fluorene, and Cyclic Urea Moieties

Cheng-Po Kuo,^{1,2} You-Shiang Lin,^{1,2} Man-kit Leung^{1,2}

¹Department of Chemistry, National Taiwan University, Taipei, Taiwan, Republic of China

²Institute of Polymer Science and Engineering, National Taiwan University, Taipei, Taiwan, Republic of China

Correspondence to: M.-k. Leung (E-mail: mkleung@ntu.edu.tw)

Received 27 June 2012; accepted 18 August 2012; published online

DOI: 10.1002/pola.26354

ABSTRACT: The study of the electrochemical fluorescence switching properties of the conjugated copolymers containing fluorene, triphenylamine, and 1,3-diphenylimidazolidin-2-one moieties is reported. The polymers show high fluorescence quantum yields, excellent thermal stability, and good solubility in polar organic solvents. While the polymer emits blue light under UV irradiation, the fluorescence intensity is quenched upon electrochemical oxidation. The fluorescent behavior can be reversibly switched between nonfluorescent (oxidized) state

and strong fluorescence (neutral) state with a high contrast ratio (I_f/I_{f0}) of 16.3. The role of the electrochemical oxidation of the triphenylamine moieties is to generate the corresponding radical cations that lead to fluorescence quenching in the solid matrix. © 2012 Wiley Periodicals, Inc. *J. Polym. Sci. Part A: Polym Chem* 000: 000–000, 2012

KEYWORDS: conjugated polymers; copolymerization; electrochemistry; fluorescence

INTRODUCTION Organic π -conjugated polymers are increasingly adaptable to many fluorescence-based chemical and biological applications.^{1,2} The ability of these conjugated polymers to amplify their sensitivity on fluorescence responses is attributed to the efficient electronic delocalization and rapid transport of excitons along the π -conjugated backbone. Much research has been done on polyureas due to their outstanding thermal and mechanical properties.^{3–9} However, to our knowledge, fabrication of solid-state electrofluorescent devices (EFD) using PU based materials has not been examined and reported. Electrofluorescent (EF) materials display a reversible optical change in the fluorescence resulting from electrochemical oxidation or reduction. Materials such as organic/inorganic hybrid thin films,¹⁰ organic metal complexes,^{11–14} organic molecules,^{15,16} and fluorescent polymers^{17,18} have been explored. In addition, fluorescence emission shows high sensitivity on response to environmental conditions. Because of these interesting properties, the redox fluorescence switching has been subject of research for potential applications such as fluorescent imaging, sensors, displays, spectroscopy, and many other optoelectronic applications.^{10–26}

A pioneer example of the solid-state EFD that switches the fluorescence by changing the redox states of tetrazine molecule, between its neutral state and an anion-radical state, was reported by Kim et al.¹⁵ The structure of the EFD was composed of ITO electrode/a blend of electroactive tetrazine

in a polymer electrolyte/photocured polymer electrolyte/ITO electrode. Upon reduction, the highly fluorescent tetrazine molecules were reduced to their nonemissive anion-radical state; the fluorescent emission from EFD was then quenched in this state. The EF process was reversible so that the device on/off could be controlled with the applied electrical potential. The EFD concept could be extended to fluorescent polymers such as poly(methylene anthracene)¹⁷ and *s*-triazine-bridged *para*-phenylenevinylene,¹⁸ so that the fluorescence properties could be electrochemically tuned. However, due to the poor miscibility of many fluorescent polymers with polymeric electrolytes, the EFD applications are limited. Recently, a novel n-type doping poly(oxadiazole) (POD)²⁶ that enables easy fabrication of EFD has been reported. The POD exhibits a reversible change in the fluorescence properties by repetitive transformation between its reduced state (nonfluorescent) and the neutral state (fluorescent) with a maximum on/off ratio of 2.5.

Complementary to the electron-deficient properties of POD, triarylamines (TAAs) are considered as a family of electron-rich materials that play an important role in optoelectronics. First, TAAs can be easily doped by oxidation to form stable radical cations. In addition, TAAs usually show good hole-transporting properties so that they are frequently adopted in the hole-transporting layers in organic electroluminescent devices. Furthermore, TAAs usually demonstrate a noticeable change of coloration upon electrochemical redox processes

Additional Supporting Information may be found in the online version of this article.

© 2012 Wiley Periodicals, Inc.

so that they can be applied in electrochromic devices.^{27–39} In addition, most of these polymers show good solubility in organic solvents due to their nonplanar propeller-shaped triarylamine units that disrupt the packing of aromatic rings in solid state; this leads to a relatively low crystallinity of the materials so that they can form homogeneous amorphous films in large-area thin-film devices, either by thermal vacuum deposition or by spin-coating methods.

The family of fluorene-based conjugated polymers (PFs) has generated interest as blue-emitting materials because of their excellent thermal stability and high fluorescence quantum yields in solution and in solid state. However, it is difficult to maintain long-term morphological stability of thin films due to crystallization or phase separation. Several methods have been used to overcome this drawback, such as introduction of bulky groups at the C-9 position of the fluorene, copolymerization with other electroactive monomers, and optimization of EL device configurations.^{40–51} We expect that modification of the PFs by introduction of cyclic urea and propeller-shaped triphenylamine units into the polymer backbone can increase morphological stability.

Polyurethanes and polyureas (PUs) form an important family of industrial polymers that have been widely used due to their good properties such as elasticity, flexibility, thermal stability, and excellent chemical resistance.^{52–58} In addition, PU conducting polymers have recently been developed^{59–61} and applications of PUs on PLED have been reported. For example, PUs can be used as effective hole-transport matrix^{62–65} as well as applied for light emitting layers.^{66–68} Traditional methods for PU synthesis usually involve diamine and diisocyanate moieties, which are toxic reagents. In this study, we report the synthesis of our target PUs of **1** and **2** (Scheme 1) through a two-step sequence from a combination of **3–6**. The use of toxic diisocyanate reagent can be avoided. In addition, we successfully fabricated an electrochemical fluorescence switching device of **2**, containing triphenylamine, fluorene, and cyclic urea moieties.

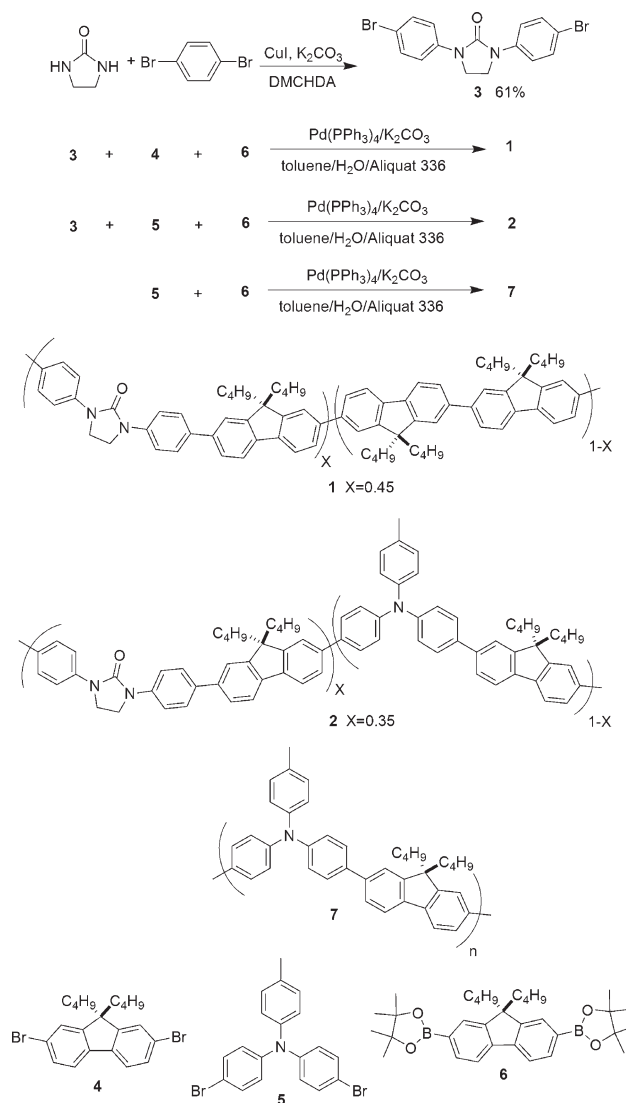
EXPERIMENTAL

Materials

All reagents, including poly(9,9-di-*n*-octylfluorene-2,7-diyl) (PDOF), imidazolidin-2-one, 1,4-dibromobenzene, diphenylamine, 4-bromotoluene, Cu powder, CuI, *N*-bromosuccinimide, Aliquat 336, and K₂CO₃ were commercially available. *trans-N, N'*-Dimethylcyclohexane-1,2-diamine (DMCHDA)⁶⁹ was synthesized according to literature procedures.

Monomer Synthesis

2,7-Dibromo-9,9-dibutylfluorene (**4**)⁷⁰ and 2,7-bis(4,4,5,5-tetramethyl-1,3,2-dioxaborolan-2-yl)-9,9-dibutylfluorene (**6**)⁷¹ were synthesized according to literature procedures. 4-Bromo-*N*-(4-bromophenyl)-*N*-*p*-tolylaniline (**5**) was synthesized according to the Supporting Information. All of the monomers were carefully purified prior to use in the polymerization reaction.



SCHEME 1 Synthetic routes of **1**, **2**, and **7**.

1,3-Bis(4-bromophenyl)imidazolidin-2-one (**3**)

To a two-necked flask were charged imidazolidin-2-one (0.75 g, 8.7 mmol), 1,4-dibromobenzene (10.2 g, 43.5 mmol), K₂CO₃ (3.0 g, 22 mmol), DMCHDA (0.49 g, 3.5 mmol), and CuI (0.33 g, 1.7 mmol) under argon. The mixture was refluxed at 120 °C for 24 h. After reaction, the mixture was cooled to room-temperature and extracted with methylene chloride and water. The separated organic layer was dried over anhydrous MgSO₄, and the solvent was evaporated. The residue was stirred for 2 h in hexane (200 mL). The resulting precipitate was collected by filtration, washed with hexane, and then dried. The crude product was purified by column chromatography, using hexane/CH₂Cl₂ (1:1) as the eluent, followed by recrystallization from CHCl₃ to afford **3** (2.1 g, 61%) as white crystals. ¹H NMR (400 MHz, CDCl₃, δ, ppm): 7.46 (s, 8H), 3.94 (s, 4H). ¹³C NMR (100 MHz, CDCl₃, δ, ppm): 131.10, 118.86, 41.64. HRMS (FAB): calcd for C₁₅H₁₂Br₂N₂O, 393.9316 (M⁺); found, 393.9307. Anal. calcd

for $C_{15}H_{12}Br_2N_2O$: C, 45.49; H, 3.05; N, 7.07. Found: C, 45.49; H, 3.38; N, 7.13.

Synthesis of Copolymer 1

To a degassed solution of **3** (0.76 g, 1.9 mmol), **4** (0.83 g, 1.9 mmol), and **6** (2.0 g, 3.8 mmol) in toluene (30 mL), K_2CO_3 (aq) (2.0 M, 15 mL), Aliquat 336 (30 mg), and tetrakis(triphenylphosphine)palladium (65.4 mg, 1.47 mol %) were added under nitrogen atmosphere. The solution was then refluxed at 90 °C for 3 days. At the end of the condensation copolymerization, the mixture was cooled and poured into a mixture of MeOH and water (300 mL, 7:3 v/v). The crude polymer was collected, washed with excess MeOH, dissolved in CH_2Cl_2 , and then reprecipitated into MeOH. Finally, the polymer was washed with acetone for 24 h using a Soxhlet apparatus, and dried under vacuum to give **1** (1.23 g, 60%). 1H NMR (400 MHz, $CDCl_3$, δ , ppm): 7.82–7.58 (m, 26H), 4.08 (br, 4H), 2.12 (br, 12H), 1.17–1.15 (br, 12H), 0.77–0.70 (br, 30H). ^{13}C NMR (100 MHz, $CDCl_3$, δ , ppm): 154.94, 151.82, 140.43, 140.04, 139.86, 139.35, 139.20, 136.36, 128.78, 127.54, 127.18, 126.10, 125.71, 121.46, 121.19, 119.99, 118.40, 74.38, 55.27, 55.23, 44.77, 42.05, 40.24, 26.13, 23.10, 13.83. Anal. Calcd for $C_{87}H_{95}N_2O$: C, 88.20; H, 8.08; N, 2.36. Found: C, 85.81; H, 7.82; N, 2.23.

Synthesis of Copolymer 2

To a degassed solution of **3** (0.76 g, 1.9 mmol), **5** (0.80 g, 1.9 mmol), and **6** (2.0 g, 3.8 mmol) in toluene (30 mL), K_2CO_3 (aq) (2.0 M, 15 mL), Aliquat 336 (30 mg), and tetrakis(triphenylphosphine)palladium (65.4 mg, 1.47 mol %) were added under nitrogen atmosphere. The reaction mixture was then refluxed at 90 °C for 3 days. At the end of the condensation polymerization, the mixture was cooled and poured into a mixture of MeOH and water (300 mL, 7:3 v/v). The crude polymer was collected, washed with excess MeOH, dissolved in CH_2Cl_2 , and then reprecipitated into MeOH. Finally, the polymer was washed with acetone for 24 h using a Soxhlet apparatus, and dried under vacuum to give **2** (1.25 g, 54%). 1H NMR (400 MHz, $CDCl_3$, δ , ppm): 7.77–7.37 (m, 20H), 7.26–7.16 (m, 12H), 4.03 (br, 4H), 2.38–2.36 (br, 3H), 2.09 (br, 8H), 1.14 (br, 8H), 0.74–0.71 (br, 20H). ^{13}C NMR (100 MHz, $CDCl_3$, δ , ppm): 154.26, 151.02, 146.48, 144.37, 139.23, 138.85, 135.77, 134.94, 132.77, 129.66, 128.37, 127.34, 127.09, 126.76, 125.29, 125.12, 124.82, 123.36, 120.70, 120.50, 119.60, 117.99, 55.29, 42.20, 40.56, 26.40, 23.47, 21.30, 14.30. Anal. Calcd for $C_{110}H_{108}N_4O$: C, 88.08; H, 7.27; N, 3.59. Found: C, 86.93; H, 7.29; N, 3.24.

Synthesis of Copolymer 7

To a degassed solution of **5** (0.8 g, 1.9 mmol) and **6** (1.0 g, 1.9 mmol) in toluene (15 mL), K_2CO_3 (aq) (2.0 M, 7.5 mL), Aliquat 336 (15 mg), and tetrakis(triphenylphosphine)palladium (32.7 mg, 1.47 mol %) were added under nitrogen atmosphere. The reaction mixture was refluxed at 90 °C for 3 days. At the end of the polymerization, the mixture was cooled and poured into MeOH in water (150 mL, 7:3 v/v). The crude polymer was collected, washed with excess MeOH, dissolved in CH_2Cl_2 , and reprecipitated into MeOH. Finally, the polymer was washed with acetone for 24 h using a Sox-

let apparatus, and dried under vacuum to give **7** (0.52 g, 50%). 1H NMR (400 MHz, $CDCl_3$, δ , ppm): 7.75–7.47 (m, 6H), 7.23–7.13 (m, 12H), 2.36 (br, 3H), 2.03 (br, 4H), 1.12–1.08 (br, 4H), and 0.71–0.59 (br, 10H).

Fabrication of Electrofluorescent Switching Devices

An EF polymer film was prepared by spin coating a solution of the **2** (10 mg mL^{-1} in $CHCl_3$) onto an ITO-coated glass substrate and then dried in vacuum.⁷² In our study, this layer also possessed a switching mechanism as well as photoluminescence. On the other layer, a gel electrolyte based on PMMA (M_w : 102,600) and $LiClO_4$ was plasticized with propylene carbonate to form a highly transparent and conductive gel. PMMA (1 g) was dissolved in dry acetonitrile (MeCN) (5 g), and $LiClO_4$ (0.1 g) was added to the polymer solution as supporting electrolyte. Then, after propylene carbonate (1.5 g) was added as plasticizer, the mixture was slowly heated until gelation. The gel electrolyte was spread on the polymer-coated side of the ITO electrode, and the electrodes were sandwiched. Finally, the device was sealed with epoxy resin.

Measurement

1H and ^{13}C NMR spectra were recorded on a Varian Unity Plus 400 MHz spectrometer. Molecular weights and polydispersities of polymers were determined by gel permeation chromatography (GPC) analysis relative to polystyrene calibration (Waters Styragel columns of HR3 and HR4E) using THF as eluent at a flow rate of 1.0 $mL\ min^{-1}$. Differential scanning calorimetry (DSC) analysis was performed under nitrogen at a heating rate of 10 °C min^{-1} . Thermogravimetric analysis (TGA) was determined under nitrogen by measuring weight loss while heating at a rate of 10 °C min^{-1} . Photoluminescence spectra were obtained on a Hitachi F-4500 luminescence spectrometer.

RESULTS AND DISCUSSION

Synthesis and Characterization of 1, 2, and 7

The synthetic routes for **1**, **2**, and **7** are shown in Scheme 1. 1,3-Bis(4-bromophenyl)imidazolidin-2-one (**3**), which was synthesized using copper (I) iodide catalyzed Goldberg–Buchwald–Nandakumar C–N coupling reactions,⁷³ was used as a starting material for the preparation of **1** and **2**. The reaction proceeded smoothly under the modified conditions of using larger amounts of CuI (20 mol %) under solvent-free condition, which gave **3** in an acceptable yield (61%). In addition, excessive 1,4-dibromobenzene (5 equiv) was used to suppress the linear polymerization between 1,4-dibromobenzene and imidazolidin-2-one.

Polymers **1** and **2** were synthesized by the Suzuki coupling reaction.⁷⁴ The copolymerization was carried out using $Pd(PPh_3)_4$ as the catalyst in a mixture of PhMe and aqueous K_2CO_3 (2.0 M) with Aliquat 336 as a phase transfer reagent. In the synthesis of **1**, a feeding ratio of 1:1:2 for **3**, **4**, and **6** was respectively adopted. The same feeding ratio for **3**, **5**, and **6** was adopted in the preparation of **2**.

Polymers **1** and **2** were characterized by 1H , ^{13}C NMR, elemental analysis, and IR spectroscopy (see Supporting

TABLE 1 Polymerization Results and Characterization of the Copolymers

Polymer	M_n^a ($\times 10^4$)	M_w^a ($\times 10^4$)	PDI ^a	T_g (°C)	T_d^b (°C)
1	0.77	1.42	1.84	178	453
2	1.32	2.80	2.12	270	395
7	1.54	8.53	5.53	246	440

^a M_n , M_w , and PDI of the polymers were determined by gel permeation chromatography using polystyrene standards in THF.

^b Temperature resulting in a 5% weight loss based on the initial weight.

Information). Both polymers were soluble in common organic solvents, such as CHCl_3 , PhMe, and THF at room temperature. Their molecular weight data and thermal properties are summarized in Table 1. The weight-average molecular weight (M_w) of 1.42×10^4 and 2.80×10^4 for **1** and **2**, with the polydispersity index (PDI) of 1.84 and 2.12, respectively, were found. The TGA analyses of **1** and **2** show a high onset of the weight-loss temperatures at 453 and 395 °C, respectively, indicating that the polymers are thermally stable (Fig. 1). In addition, DSC curves of **1** and **2** also display high glass transition temperatures (T_g) of 178 and 270 °C respectively, which are much higher than that of **PDOF** (reported to be about 75 °C).⁷⁵

Figure 2 shows the ^1H NMR of **1** and **2**. The composition of **1** was characterized on the basis of the signal intensities at δ 4.08 and 2.12, which were respectively assigned to the ethylene protons of the imidazolidin-2-one and the 1-methylene protons on the butyl side-chains of the fluorene moieties. The area ratio of 1:3.40 was obtained in the spectrum, indicating that a ratio of 1:1.2:2.2 for **3:4:6**, respectively, was incorporated in the condensation copolymerization. This value is consistent with the monomer-feeding ratio of 1:1:2. The values of the fraction of the basic units of 0.45 and 0.55 for (x) and ($1 - x$) respectively, shown in the formula of **1** in Figure 2, were then calculated.

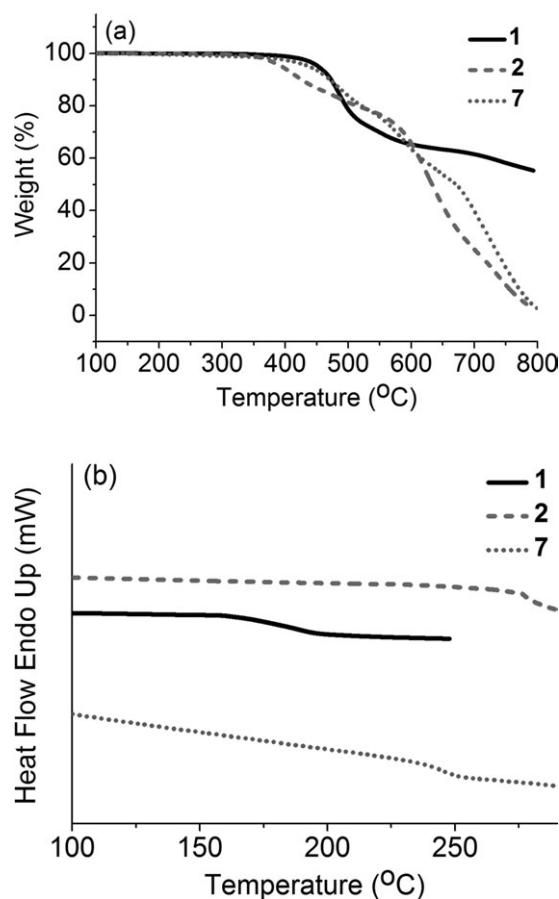
However, the composition of **2** was established on the basis of the integrations of 4.0:5.6:11.3 at δ 4.03, 2.37, and 2.09 respectively. While the signals at δ 4.03 and 2.09 were assigned as before, the sharp singlet at δ 2.37 was assigned to the methyl protons on the tolyl group of the triphenylamine units. The integration ratio suggests that a ratio of 1:1.9:2.9 for **3:5:6**, respectively, was incorporated. Even though the reason is still unclear, the above results suggested that the monomer **5** is more reactive than **3** and preferentially incorporated in the condensation copolymerization with **6**. The fraction of 0.35 and 0.65 for (x) and ($1 - x$) respectively, shown in the formula of **2** in Figure 2, were then estimated.

To make a comparison, copolymer **7** was included as reference in our study. Therefore, we prepared copolymer **7** from **5** and **6** (1:1) according to the same Suzuki coupling protocol. However, as shown in the GPC (Fig. 3), the Suzuki coupling reaction of **5** and **6** led to a polymeric product with bimodal distribution. The number-average molecular weight

(M_n) of 1.54×10^4 , with the PDI of 5.53, was recorded. The bimodal distribution pattern is unexpected and has not been observed in the preparation of **1** and **2**. Nevertheless, the ^1H NMR integration suggests that a ratio of 1:1 for **5** and **6** was incorporated in **7**. The TGA analysis of **7** shows a high onset of the weight-loss temperature at 440 °C. In addition, DSC curve of **7** also displays high glass transition temperature (T_g) of 246 °C (Fig. 1).

Optical Properties

UV-vis and photoluminescence spectra of **1** and **2** in CHCl_3 or in thin film on quartz plates are shown in Figure 4. The data are summarized in Table 2. The UV-vis spectrum of **1** in CHCl_3 shows an absorption band peaking at about 366 nm, which is corresponding to the π - π^* electronic transitions in the conjugated polyfluorene chromophore [Fig. 4(a)]. However, in comparison to that of **PDOF**, the absorption spectrum of **1** is blue-shifted by 20 nm. This result suggests that inserting cyclic urea units onto the polyfluorene backbone interrupts the linear π -conjugation. However, the solution of **2** in CHCl_3 displays an absorption band peaking at about 360 nm, which is corresponding to the π - π^* transitions of the fluorene units. In addition, **2** shows a shoulder band peaking at about 300 nm that is mostly attributed to the absorption of the triphenylamine moieties.

**FIGURE 1** (a) TGA and (b) DSC thermograms of **1**, **2**, and **7**.

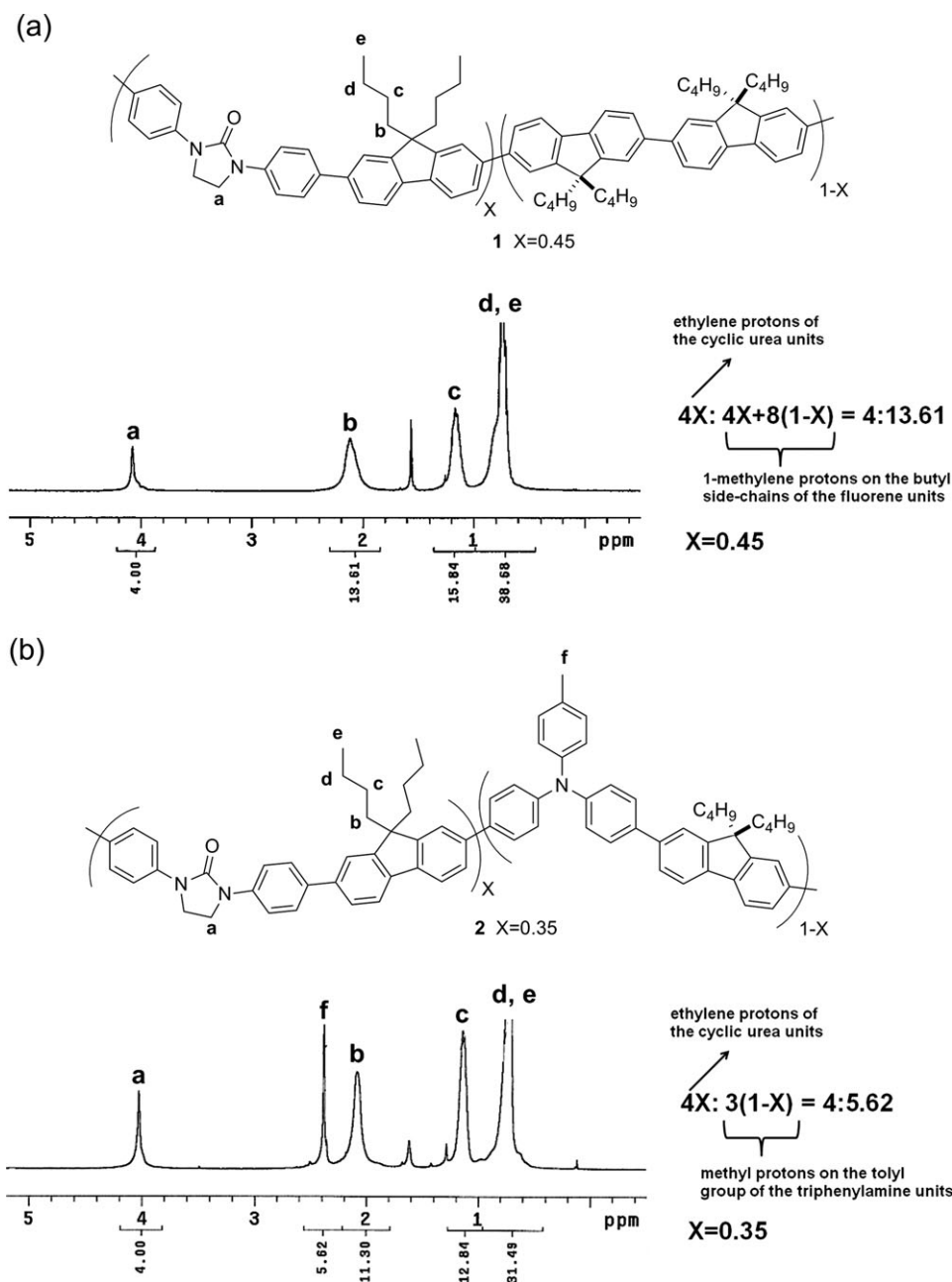


FIGURE 2 ^1H NMR spectra of (a) **1** and (b) **2**.

Compared with that of **1**, the absorption maximum of **2** is slightly blue-shifted by 6 nm, suggesting that the conjugated length of fluorene units of **2** is shorter. This is reasonable because one might expect that the fluorene moieties be separated either by the cyclic urea or by the triphenylamine moieties on **2**.

However, **7** shows two absorption bands; one peaking at 386 nm while the other peaking at 300 nm. The absorption band at 386 nm overlaps with that of **PDOF**, indicating that this absorption is arising from the fluorene chromophore. However, the shoulder band peaking at about 300 nm is attributed to the absorption of the triphenylamine moieties.

Under UV irradiation, **1**, **2**, and **7** show strong PL in CHCl_3 . As shown in Figure 4(a), even though the conjugated length of **1** is expected to be different from that of **PDOF** in ground state, polymer **1** shows a blue emission peaking at 415 nm that is almost identical to that of **PDOF**. In addition, both emission spectra present similar vibronic fine patterns, which are characteristic for rigid π -conjugated systems. On the contrary, polymers of **2** and **7** show relatively broad and red-shifted emission bands peaking at 432 and 434 nm, respectively. The PL quantum yields (Φ_{PL}) of 0.87, 0.82, and 0.65 were respectively estimated for **1**, **2**, and **7**, by comparing against Coumarin 1 ($\Phi_{\text{PL}} = 0.85$) as the standard.⁷⁶

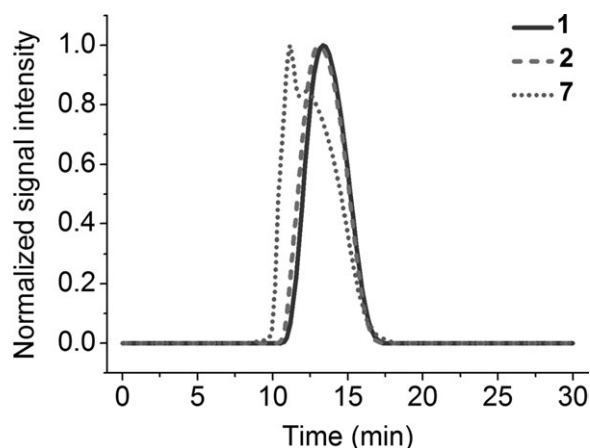


FIGURE 3 GPC of **1**, **2**, and **7**.

Figure 4(b) shows the UV-vis and PL spectra of the polymers in the solid-film state. The absorption spectra of the polymers in the solid-film state are similar to those in CHCl_3 . The absorption maximum of **1**, **2**, and **7** at 365, 358, and 376 nm respectively, are attributed to the π - π^* electronic transitions in the conjugated fluorene chromophore.

The emission maximum of **1** and **2** were recorded at 423 and 443 nm, respectively. More importantly, the PL spectra of **1** and **2** in the solid-film state were found to be almost identical to those in dilute CHCl_3 , indicating that the intermolecular interactions in the solid state are negligible. By comparing against the fluorescence intensity of **PDOF** thin-film sample ($\Phi_{\text{PL}} = 0.55$),⁷⁷ the PL quantum yields of 0.77 and 0.73 for **1** and **2**, respectively, were found. Although the emission maximum of **7** in the solid-film state is almost identical with that in dilute CHCl_3 , vibronic pattern is clearly observed in the solid-film state spectrum. The PL quantum yield of 0.43 is much lower than that of **1** and **2**.

To examine the thermal effects on the optical behavior, the thin films of **1**, **2**, **7**, and **PDOF** were heated at 220 °C under nitrogen for 40 min (Fig. 5). After thermal treatment, the PL spectra of the thin film of **1**, **2**, and **7** remained almost unchanged. These results indicate that the thin films are morphologically stable. Although we cannot provide any rationale about this effect in this stage, this observation clearly suggested that introduction of the cyclic urea and triphenylamine moieties can effectively suppress π -stacking/aggregation of the conjugated polymers in the solid state. However, the PL spectrum of the annealed **PDOF** film is red shifted by 10 nm with the excimer emission peaking at 520 nm being observed.^{78,79} This observation again implies that introduction of cyclic urea and the triphenylamine units can increase the morphological stability of the film at high temperature.

Electrochemical Properties

The redox behavior of the polymers was investigated by cyclic voltammetry (CV) in tetrabutylammonium perchlorate (TBAP)/ CH_2Cl_2 (0.1 M/10 mL), using a Pt electrode as the work electrode, a Pt wire as the counter electrode, and an Ag/AgCl couple as the reference. The scan rate being adopted was

100 mV/s. Figure 6(a) shows the cyclic voltammograms of **1**, **2**, and **7** (5 mg) in the supporting electrolyte of TBAP/ CH_2Cl_2 (0.1 M). Polymers **2** and **7** show one reversible oxidation wave at $E_{1/2}(\text{Ox}) = 0.88$ V, which is attributed to the electrochemical oxidation of the triphenylamine units to the cation radicals. The second wave shows up after 1.2 V. In addition, polymer **1** has an onset voltage at 1.15 V. The HOMOs of -5.48 and -5.12 eV for **1** and **2**, respectively, were therefore estimated with regard to the energy level of the ferrocene reference (4.8 eV below the vacuum level). The LUMOs of -2.46 and -2.17 eV for **1** and **2**, respectively, were then calculated from the HOMO energy level and the optical band gap.

CV of the polymer films coated on an ITO electrode was performed in an electrolyte of TBAP/acetonitrile (MeCN) (0.1 M) [Fig. 6(b)]. We intentionally picked out MeCN as the solvent for two reasons: (1) the polymer films are insoluble in MeCN; (2) MeCN is a polar aprotic solvent that benefits the electrochemical oxidation process. The polymer films were prepared by spin coating the solution of **1** and **2** (10 mg mL^{-1} in CHCl_3) on ITO-coated glass substrates and then dried in vacuum. As shown in Figure 6(b), the oxidation of **1** has an onset at 1.19 V with an anodic wave peaking at 1.48 V. The oxidation is quasi-reversible with the corresponding cathodic current peaking at 1.25 V. However, **2** and **7** are oxidized at 0.82 V, followed by the second and the third waves

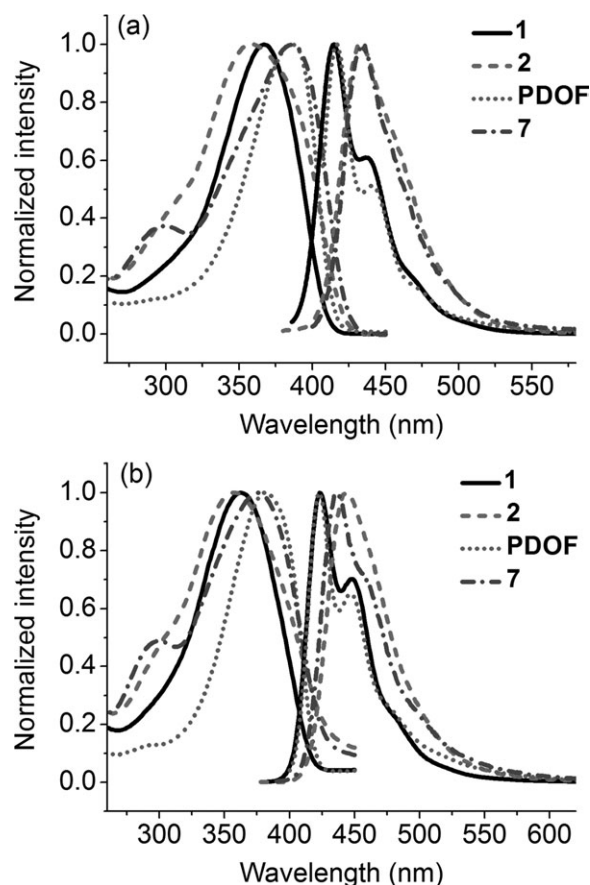


FIGURE 4 UV-vis absorption and PL spectra of **1**, **2**, **PDOF**, and **7** in (a) CHCl_3 solution and (b) solid-film state.

TABLE 2 Optical Properties of the Copolymers

Polymer	Solution			Film		
	Abs (nm) λ_{\max}	PL (nm) λ_{\max}	$\Phi_{\text{PL}}^{\text{a}}$	Abs (nm) λ_{\max}	PL (nm) λ_{\max}	$\Phi_{\text{PL}}^{\text{b}}$
1	366	415	0.87	365	423	0.77
2	360	432	0.82	358	443	0.73
7	386	434	0.65	376	435	0.43
PDOF	386	417	0.78	382	423	0.55

^a Coumarin 1 ($\Phi_{\text{PL}} = 0.85$)⁷⁶ as the standard in THF solution.

^b Poly(9,9-dioctylfluorene) ($\Phi_{\text{PL}} = 0.55$)⁷⁷ as the standard in thin-film state.

after 1.2 V. When the CV scan was swept from 0 V to 1 V, **2** and **7** showed a strong oxidation wave with an onset at 0.80 V. However, **1** showed only a very weak residual current, indicating that the triphenylamine moiety can be preferentially oxidized over the fluorene and the imidazolidin-2-one moieties under the CV condition.

Electrochemical Redox Switching of Fluorescence

In preliminary study, the polymer films used in the experiments of fluorescence intensity changes were prepared by spin coating the solution of copolymers **1** and **2**

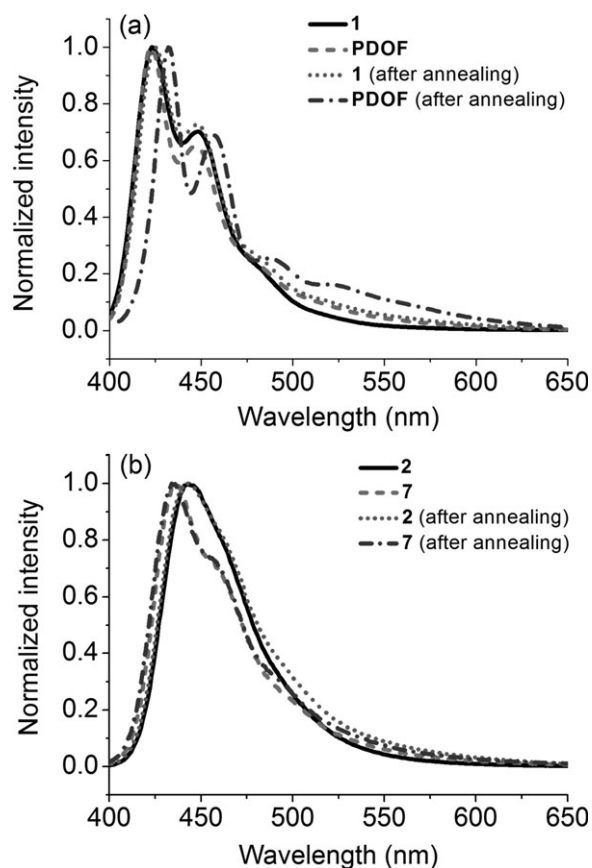


FIGURE 5 Comparison of the PL spectra of (a) **1** and PDOF; (b) **2** and **7**, before and after annealing at 220 °C for 40 min under nitrogen.

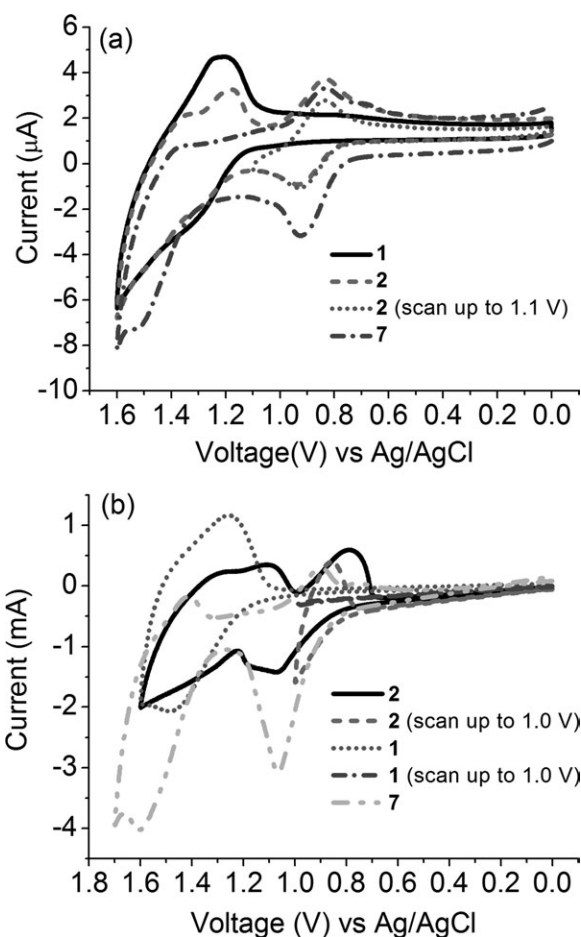


FIGURE 6 (a) CV of **1**, **2**, and **7** in TBAP/CH₂Cl₂ (0.1 M); (b) CV of the films of **1**, **2**, and **7** on an ITO-coated glass substrate in TBAP/MeCN (0.1 M). The scan rate was 100 mV/s.

(10 mg mL⁻¹ in CHCl₃) onto an ITO-coated glass substrate. The films were highly fluorescent in the blue to sky-blue region. The electrochemical oxidation was performed in TBAP/MeCN (0.1 M) with the applied electrical potential of 1.0 V that led to fluorescence decrease for **1** and **2** (Fig. 7). The fluorescence intensity changes were collected every 1 min. The fluorescence intensity of **2** was completely quenched after 1.0 min of oxidation. However, the fluorescence intensity of **1** was reduced to only half of its original intensity after electrochemical oxidation for 5 min. This result suggests that fluorescence of **2** can be quenched more effectively than **1** during oxidation.

To test the possibility of using **1** and **2** as an EF switching material, we had subjected the polymers to repetitive CV-sweeps in which the fluorescence intensity of the polymers were simultaneously followed (Fig. 8). The studies were carried out under similar conditions as described above, with the polymer coated on ITO glass. The sweep was set between 0 and 1 V with a scan rate of 100 mV/s. TBAP/MeCN (0.1 M) was adopted as the supporting electrolyte.

Upon electrochemical oxidation, the bright fluorescence of **2** was gradually reduced and completely quenched at 1.0 V.

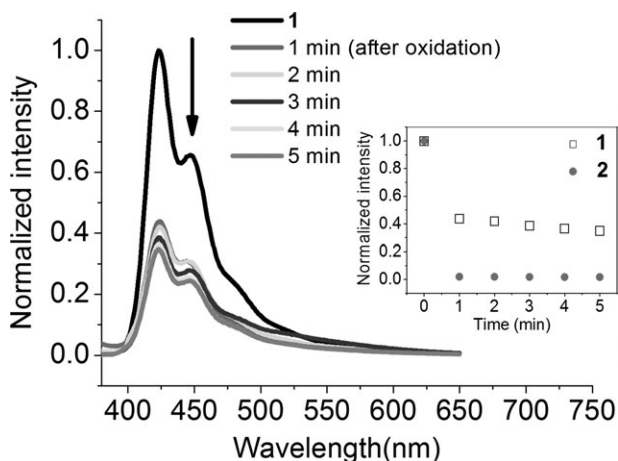


FIGURE 7 Fluorescence intensity changes ($\lambda_{\text{exc}} = 365 \text{ nm}$) of the film of **1** on an ITO-coated glass substrate were carried out in TBAP/MeCN (0.1 M) after applying an oxidation potential of 1.0 V (vs. Ag/AgCl) at different times (min). Inset: Comparison of the fluorescence intensity changes (Normalized) of **1** and **2** at 423 and 443 nm, respectively, versus time (min).

However, the quenching process is reversible so that the fluorescence intensity of **2** can be gradually resumed to the original emission intensity (>95%) in the reverse-sweep.

On the contrary, the intensity of the bright fluorescence of **1** only slightly altered upon electrochemical oxidation. However, the process is only partially reversible so that about 40% of the original fluorescence loss can be recovered after the first CV cycle. The maximum intensity gradually drops after each cycle, indicating that the film is unstable upon electrochemical oxidation. Since polymer **1** may contain oligofluorene segments with various conjugation lengths, we tentatively attribute the partial quenching phenomenon to electrochemical oxidation occurring on the long oligofluorene segments. First, the longer the conjugation length of the segment, the lower the oxidation potential it possesses. In addition,

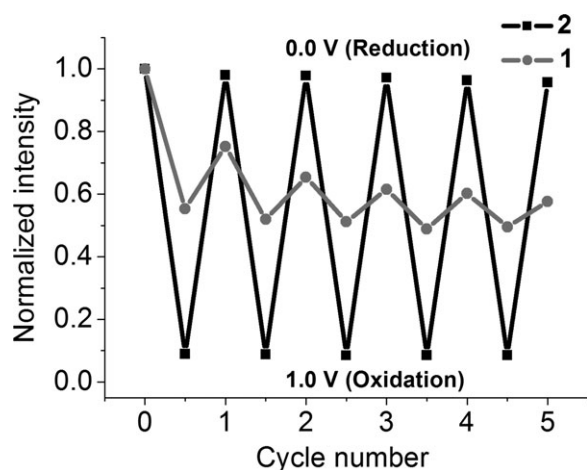


FIGURE 8 Fluorescence intensity changes of the films of **1** and **2** on ITO were carried out by CV for five scanning-cycles. The fluorescence intensity changes at 0.0 V (reduction) and 1.0 V (oxidation) were recorded.

tion, as we mentioned in Figure 6(b), even though the anodic current of **1** below 1 V was small, a residual current was still observed in the CV, which supports this hypothesis.

EF switching of the film of **7** on an ITO-coated glass substrate in the supporting electrolyte of TBAP/MeCN (0.1 M) can also be observed by chronoamperometric analysis. However, for unknown reasons, the EF switching processes proceeded less effectively and unevenly on the ITO electrode. Figure 9 shows how the quenching process of the blue-light emission evolved. After an electrical potential of 0.9 V was applied, the fluorescence quenching was started to occur at the right-bottom corner [Fig. 9(b)], gradually extended to the central part of the plate after 1 s [Fig. 9(c)] and reached the quenched state after 3 s [Fig. 9(d)].

Proposed mechanisms of the oxidative fluorescence quenching process of **2** are illustrated in Scheme 2. When an electrical potential set below 1.0 V was applied, oxidation selectively occurred on the triphenylamine moieties and gave rise to the corresponding radical cations. Since the radical cation is known to have a strong absorption in the blue-light region,²⁹ it acts as an effective fluorescence quencher so that the photoluminescence of **2** is efficiently quenched. When a reverse sweep was applied, the triphenylamine radical cations in **2** were annihilated and the fluorescence at a neutral state of **2** was recovered. Perhaps due to the dipolar properties of the ureylene groups that could help to stabilize the formation of the triphenylamine radical cations, the redox fluorescence switching of **2** is more effective than **7**.

The durability of the potential-dependent switchable fluorescence properties of **2** was investigated by chronoamperometric

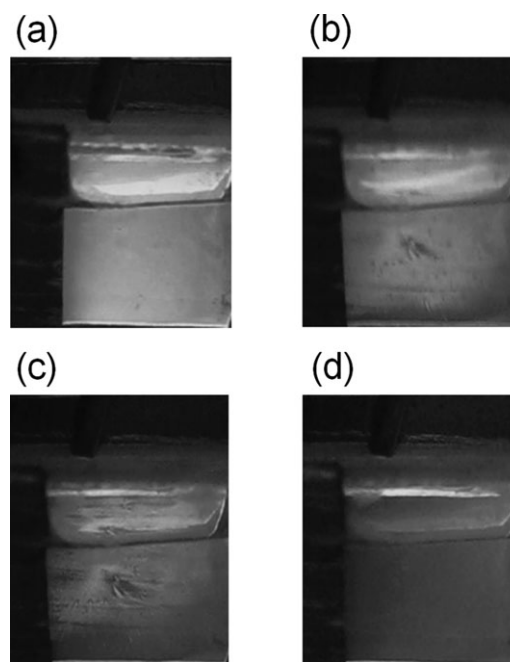
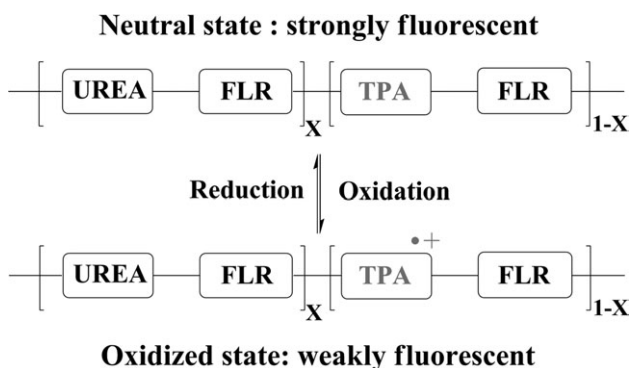


FIGURE 9 EF switching of the film of **7** on ITO after an electrical potential of 0.9 V was applied: (a) Before oxidation. (b) After oxidation for 0.5 s. (c) After oxidation for 1 s. (d) After oxidation for 3 s.



SCHEME 2 Illustration of the EF switching based on a copolymer of **2**.

analysis (Fig. 10). Twenty-five redox pulse-cycles were carried out for the thin-film of **2** in the supporting electrolyte of TBAP/MeCN (0.1 M) with fixed electrical potential steps of 0.9 V for oxidation and 0.0 V for reduction. The potential step was flipped every 3 s. Indeed, the EF switching of the thin-film of **2** was found to be responsive within 3 s with a maximum on/off ratio of 16.3. The fluorescence intensity was recovered after each step and found to be recovered rapidly and fully on completion of the step, thus, demonstrating the reversibility of the switching process.

Electrochemical Fluorescence Switching in an Electrofluorescent Device

We had fabricated a prototype of the single-layer EFD as shown in Figure 11. The thin-film of **2** was spun onto a piece of ITO-glass and dried, and a layer of gel electrolyte was spread on top. The counter electrode was then placed to

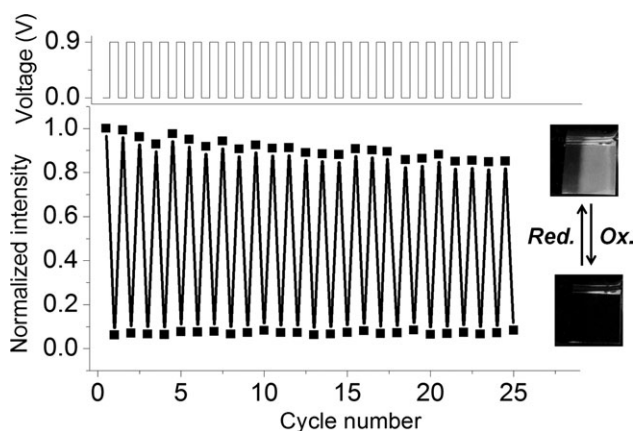


FIGURE 10 Twenty-five redox pulse-cycles of a thin-film of **2** were carried out in TBAP/MeCN (0.1 M) with fixed electrical potential steps of 0.9 V for oxidation and 0.0 V for reduction. The potential step was flipped every 3 s. All the bottom dots were detected after the thin film was oxidized at an applied potential of 0.9 V, and all the top dots were measured after the thin film was reduced at an applied potential of 0.0 V. Inset: Photographs are the image of the fluorescence changes of a thin-film of **2** at indicated potentials under UV irradiation (365 nm).

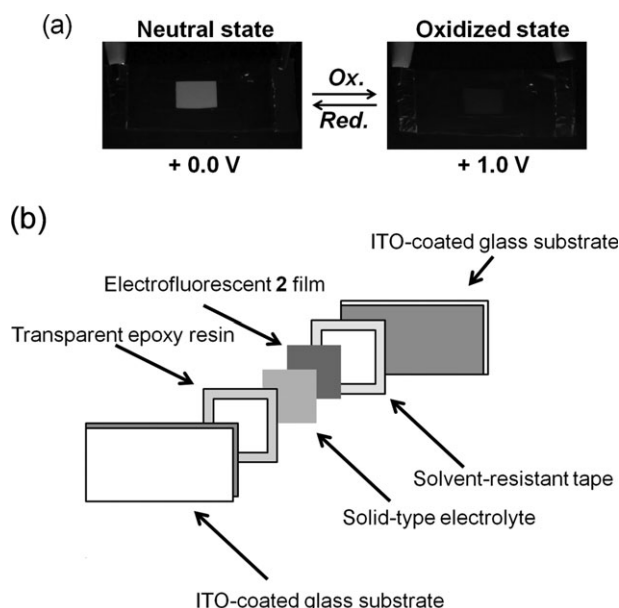


FIGURE 11 (a) Photographs of a single-layer ITO-coated glass EF device, using **2** as an active layer. Successive images of the cell fluorescence recorded at different states under UV irradiation (365 nm). (b) Schematic diagram of the **2**-EFD sandwich cell.

sandwich the electroactive layer. To prevent any electrolyte leakage, an epoxy resin was applied to seal the device. Redox pulse-cycles were carried out for the EFD of **2**. Fixed potentials at 1.0 V (for oxidation) and 0.0 V (for reduction) were used and flipped every 5 s. Before data collection, the device was pretreated with the pulse-cycles for 400 s (Fig. 12).

The polymer film showed strong fluorescence in the neutral form. When a voltage of 1.0 V was applied, the fluorescence disappeared due to electrochemical oxidation (the same

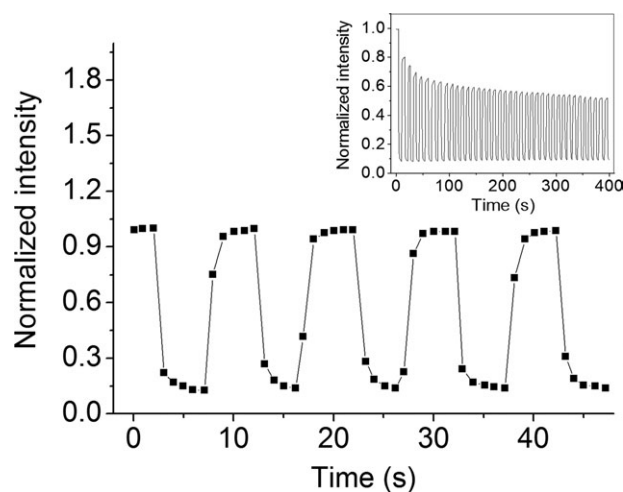


FIGURE 12 Fluorescence intensity changes ($\lambda_{\text{exc}} = 360 \text{ nm}$) of the solid-state **2**-EFD at 443 nm after 400 s of pretreatment. Fixed potentials at 1.0 V (for oxidation) and 0.0 V (for reduction) were used and flipped every 5 s. Inset: Fluorescence intensity changes of the solid-state **2**-EFD.

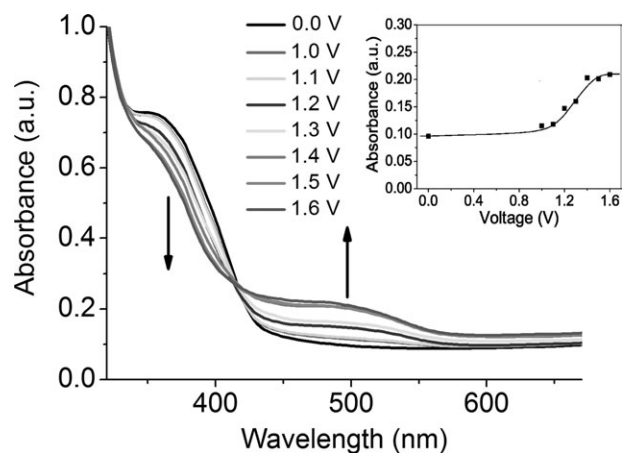


FIGURE 13 Spectroelectrochemistry of the solid-state 2-EFD. Inset: The absorption intensity changes of the solid-state 2-EFD at 500 nm versus voltage (V).

result was reported for the thin film in the previous chronoamperometric experiments). When the potential was subsequently set back at 0 V, the polymer film was turned back to the strongly fluorescent neutral state (Fig. 11).

Figure 12 demonstrates the fluorescence intensity changes of the solid-state EFD of **2**. As shown in the inset of Figure 12, although a fast response of the EFD was clearly observed, only 80% of the original fluorescence intensity was recovered in the first cycle. In the early stage, the intensity of the 2-EFD continuously dropped during operation. However, after treatment of the EFD with the electrical pulse-cycles for 400 s, the device gradually got into a steady-state. Figure 12 shows the data after 400 s of pretreatment. One can see that over 80% of the fluorescent intensity was effectively quenched within one second after the electrical potential was applied, and the fluorescence intensity could be recovered after each cycle.

To elucidate the EF switching mechanisms in the solid-state EFD of **2**, spectroelectrochemistry was employed to monitor the redox intermediates that are generated in the cell. Figure 13 displays the UV-vis spectra being collected under different applied electrical potentials for 150 s. A new absorption band peaking at 500 nm was observed when the applied electrical voltage was set to be higher than 1.0 V. The absorption intensity gradually increased with increasing the applied electrical potential, supporting our assumption of the triphenylamine radical cation formation.²⁹

CONCLUSIONS

We have successfully established a design of robust materials for EFD. In our design, by taking advantage of the high fluorescence quantum yield, we adopted fluorene moieties as our luminophore. To control the solubility of the polymer, as well as to benefit the ion transport during the electrochemical process, dipolar cyclic urea moieties were also introduced into the backbone. The electrochemically active triphenylamine-core played another key role in controlling the emis-

sive properties of **2**. On the one hand, **2** showed modest solubility in organic solvents and high T_g , which would benefit device fabrication. On the other hand, reversible fluorescence switching of **2** from a highly fluorescent neutral state to a non-fluorescent. When comparing against the fluorescence switching performance of the thin-film of **7**, one may aware that introduction of the cyclic urea moieties is particularly important for fabrication of the fast response EFD. This is probably due to the dipolar properties of the urea groups that benefit the LiClO_4 penetration. In addition, the presence of the dipolar groups may also help to reduce the barrier of the triphenylamine radical cation formation.

ACKNOWLEDGMENT

This work was supported by the Ministry of Education and National Taiwan University, National Science Council of Taiwan (NSC-98-2119-M-002-006-MY3 and 99-2119-M-002-007), and the thematic project, Academia Sinica.

REFERENCES AND NOTES

- 1 Swager, T. M. *Acc. Chem. Res.* **1998**, *31*, 201–207.
- 2 Yang, J.-S.; Swager, T. M. *J. Am. Chem. Soc.* **1998**, *120*, 5321–5322.
- 3 Grujicic, M.; He, T.; Pandurangan, B.; Svingala, F. R.; Settles, G. S.; Hargather, M. J. *J. Mater. Eng. Perform.* **2012**, *21*, 2–16.
- 4 San-José, N.; Gómez-Valdemoro, A.; Estevez, P.; García, F. C.; Serna, F.; García, J. M. *Eur. Polym. J.* **2008**, *44*, 3578–3587.
- 5 Fehervari, A. F.; Kagumba, L. C.; Hadjikyriacou, S.; Chen, F.; Gaudiana, R. A. *J. Appl. Polym. Sci.* **2003**, *87*, 1634–1645.
- 6 Hartmann-Thompson, C.; Keeley, D. L.; Rousseau, J. R.; Dvornic, P. R. *J. Polym. Sci. Part A: Polym. Chem.* **2009**, *47*, 5101–5115.
- 7 Novikova, T. S.; Barashkov, N. N.; Sakhno, T. V. *Proc. SPIE* **2003**, *5257*, 270–274.
- 8 Wang, S.-K.; Sung, C. S. P. *Macromolecules* **2002**, *35*, 883–888.
- 9 Simas, E. R.; Akcelrud, L. *J. Lumin.* **2003**, *105*, 69–79.
- 10 Wang, B.; Bi, L.-H.; Wu, L.-X. *J. Mater. Chem.* **2011**, *21*, 69–71.
- 11 Santis, G. D.; Fabbrizzi, L.; Licchelli, M.; Sardone, N.; Velders, A. H. *Chem. Eur. J.* **1996**, *2*, 1243–1250.
- 12 Martínez, R.; Ratera, I.; Tárraga, A.; Molina, P.; Veciana, J. *Chem. Commun.* **2006**, 3809–3811.
- 13 Zhang, R.; Wu, Y.; Wang, Z.; Xue, W.; Fu, H.; Yao, J. *J. Phys. Chem. C* **2009**, *113*, 2594–2602.
- 14 Casa, M. D.; Fabbrizzi, L.; Licchelli, M.; Poggi, A.; Sacchi, D.; Zema, M. *J. Chem. Soc. Dalton Trans.* **2001**, 1671–1675.
- 15 Kim, Y.; Kim, E.; Clavier, G.; Audebert, P. *Chem. Commun.* **2006**, *34*, 3612–3614.
- 16 Zhang, G.; Zhang, D.; Guo, X.; Zhu, D. *Org. Lett.* **2004**, *6*, 1209–1212.
- 17 You, J.; Kim, Y.; Kim, E. *Mol. Cryst. Liq. Cryst.* **2010**, *520*, 128–135.
- 18 Yoo, J.; Kwon, T.; Sarwade, B. D.; Kim, Y.; Kim, E. *Appl. Phys. Lett.* **2007**, *91*, 241107.
- 19 Hennrich, G.; Sonnenschein, H.; Resch-Genger, U. *J. Am. Chem. Soc.* **1999**, *121*, 5073–5074.
- 20 Browne, W. R.; Pollard, M. M.; Lange, B. D.; Meetsma, A.; Feringa, B. L. *J. Am. Chem. Soc.* **2006**, *128*, 12412–12413.

- 21 Kwon, T.; Sarwade, B. D.; Kim, Y.; Yoo, J.; Kim, E. *Mol. Cryst. Liq. Cryst.* **2008**, *486*, 101–109.
- 22 Yun, C.; You, J.; Kim, J.; Huh, J.; Kim, E. *J. Photochem. Photobiol. C* **2009**, *10*, 111–129.
- 23 Lee, W. R.; Kim, Y.; Kim, J. Y.; Kim, T. H.; Ahn, K. D.; Kim, E. *J. Nanosci. Nanotechnol.* **2008**, *8*, 4630–4634.
- 24 Jeong, Y.-C.; Yang, S. I.; Kim, E.; Ahn, K.-H. *Macromol. Rapid Commun.* **2006**, *27*, 1769–1773.
- 25 Do, J.; Huh, J.; Kim, E. *Langmuir* **2009**, *25*, 9405–9412.
- 26 Seo, S.; Kim, Y.; You, J.; Sarwade, B. D.; Wadgaonkar, P. P.; Menon, S. K.; More, A. S.; Kim, E. *Macromol. Rapid Commun.* **2011**, *32*, 637–643.
- 27 Ogino, K.; Kanegae, A.; Yamaguchi, R.; Sato, H.; Kurjata, J. *Macromol. Rapid Commun.* **1999**, *20*, 103–106.
- 28 Yu, W.-L.; Pei, J.; Huang, W.; Heeger, A. *J. Chem. Commun.* **2000**, *8*, 681–682.
- 29 Chou, M.-Y.; Leung, M.-k.; Su, Y. O.; Chiang, C. L.; Lin, C.-C.; Liu, J.-H.; Kuo, C.-K.; Mou, C.-Y. *Chem. Mater.* **2004**, *16*, 654–661.
- 30 Cheng, S.-H.; Hsiao, S.-H.; Su, T.-H.; Liou, G.-S. *Macromolecules* **2005**, *38*, 307–316.
- 31 Liou, G.-S.; Hsiao, S.-H.; Huang, N.-K.; Yang, Y.-L. *Macromolecules* **2006**, *39*, 5337–5346.
- 32 Liou, G.-S.; Hsiao, S.-H.; Chen, W.-C.; Yen, H.-J. *Macromolecules* **2006**, *39*, 6036–6045.
- 33 Chang, C.-W.; Liou, G.-S.; Hsiao, S.-H. *J. Mater. Chem.* **2007**, *17*, 1007–1015.
- 34 Liou, G.-S.; Hsiao, S.-H.; Chen, H.-W. *J. Mater. Chem.* **2006**, *16*, 1831–1842.
- 35 Liang, F.; Pu, Y.-J.; Kurata, T.; Kido, J. Nishide, H. *Polymer* **2005**, *46*, 3767–3775.
- 36 Wang, H.-M.; Hsiao, S.-H. *J. Polym. Sci. Part A: Polym. Chem.* **2011**, *49*, 337–351.
- 37 Li, Y.; Michinobu, T. *J. Polym. Sci. Part A: Polym. Chem.* **2012**, *50*, 2111–2120.
- 38 Yen, H.-j.; Guo, S.-m.; Yeh, J.-m.; Liou, G.-S. *J. Polym. Sci. Part A: Polym. Chem.* **2011**, *49*, 3637–3646.
- 39 Kung, Y.-C.; Hsiao, S.-H. *J. Polym. Sci. Part A: Polym. Chem.* **2011**, *49*, 3475–3490.
- 40 Scherf, U.; List, E. J. W. *Adv. Mater.* **2002**, *14*, 477–487.
- 41 Kreyenschmidt, M.; Klaerner, G.; Fuhrer, T.; Ashenurst, J.; Karg, S.; Chen, W. D. Lee, V. Y.; Scott, J. C.; Miller, R. D. *Macromolecules* **1998**, *31*, 1099–1103.
- 42 Pei, Q.; Yang, Y. *J. Am. Chem. Soc.* **1996**, *118*, 7416–7417.
- 43 Shu, C.-F.; Dodda, R.; Wu, F.-I.; Liu, M. S.; Jen, A. K.-Y. *Macromolecules* **2003**, *36*, 6698–6703.
- 44 Li, Y.; Ding, J.; Day, M.; Tao, Y.; Lu, J.; D'iorio, M. *Chem. Mater.* **2004**, *16*, 2165–2173.
- 45 Setayesh, S.; Grimsdale, A. C.; Weil, T.; Enkelmann, V.; Müllen, K.; Meghdadi, F.; List, E. J. W.; Leising, G. *J. Am. Chem. Soc.* **2001**, *123*, 946–953.
- 46 Tang, R.; Tan, Z.; Li, Y.; Xi, F. *Chem. Mater.* **2006**, *18*, 1053–1061.
- 47 Kim, Y.-H.; Zhao, Q.; Kwon, S.-K. *J. Polym. Sci. Part A: Polym. Chem.* **2006**, *44*, 172–182.
- 48 Zhao, Q.; Kim, Y.-H.; Dang, T. T. M.; Shin, D.-C.; You, H.; Kwon, S.-K. *J. Polym. Sci. Part A: Polym. Chem.* **2007**, *45*, 341–347.
- 49 Chen, L.; Li, P.; Tong, H.; Xie, Z.; Wang, L.; Jing, X.; Wang, F. *J. Polym. Sci. Part A: Polym. Chem.* **2012**, *50*, 2854–2862.
- 50 Shih, H.-M.; Wu, R.-C.; Shih, P.-I.; Wang, C.-L.; Hsu, C.-S. *J. Polym. Sci. Part A: Polym. Chem.* **2012**, *50*, 696–710.
- 51 Tan, H.; Yu, J.; Wang, Y.; Li, J.; Cui, J.; Luo, J.; Shi, D.; Chen, K.; Liu, Y.; Nie, K.; Zhu, W. *J. Polym. Sci. Part A: Polym. Chem.* **2012**, *50*, 149–155.
- 52 *The Polyurethanes Book*; Randall, D.; Lee, S., Eds.; Wiley: New York, **2002**.
- 53 Li, Y.; Kang, W.; Stoffer, J. O.; Chu, B. *Macromolecules* **1994**, *27*, 612–614.
- 54 Suresh, K. I.; Kishanprasad, V. S. *Ind. Eng. Chem. Res.* **2005**, *44*, 4504–4512.
- 55 Green, R. J.; Corneillie, S.; Davies, J.; Davies, M. C.; Roberts, C. J.; Schacht, E.; Tendler, S. J. B.; Williams, P. M. *Langmuir* **2000**, *16*, 2744–2750.
- 56 Hasegawa, M.; Ikawa, T.; Tsuchimori, M.; Watanabe, O.; Kawata, Y. *Macromolecules* **2001**, *34*, 7471–7476.
- 57 Crenshaw, B. R.; Weder, C. *Macromolecules* **2006**, *39*, 9581–9589.
- 58 Tovar, J. D.; Harvey, C. P. *J. Polym. Sci. Part A: Polym. Chem.* **2011**, *49*, 4861–4874.
- 59 Njuguna, J.; Pielichowski, K. *J. Mater. Sci.* **2004**, *39*, 4081–4094.
- 60 Wang, Y. Z.; Hsu, Y. C.; Chou, L. C.; Hsieh, K. H. *J. Polym. Res.* **2004**, *11*, 127–132.
- 61 Sanjai, B.; Raghunathan, A.; Natarajan, T. S.; Rangarajan, G.; Thomas, S.; Prabhakaran, P. V.; Venkatachalam, S. *Phys. Rev. B* **1997**, *55*, 10734–10744.
- 62 Kuo, C.-H.; Peng, K.-C.; Kuo, L.-C.; Yang, K.-H.; Lee, J.-H.; Leung, M.-k.; Hsieh, K.-H. *Chem. Mater.* **2006**, *18*, 4121–4129.
- 63 Ku, C.-H.; Kuo, C.-H.; Chen, C.-Y.; Leung, M.-k.; Hsieh, K.-H. *J. Mater. Chem.* **2008**, *18*, 1296–1301.
- 64 Lin, K.-R.; Kuo, C.-H.; Kuo, L.-C.; Yang, K.-H.; Leung, M.-k.; Hsieh, K.-H. *Eur. Polym. J.* **2007**, *43*, 4279–4288.
- 65 Chuang, C.-N.; Kuo, C.-H.; Cheng, Y.-S.; Huang, C.-K.; Leung, M.-k.; Hsieh, K.-H. *Polymer* **2012**, *53*, 2001–2007.
- 66 Lim, H.; Noh, J. Y.; Lee, G. H.; Lee, S. E.; Jeong, H.; Lee, K.; Cha, M.; Suh, H.; Ha, C.-S. *Thin Solid Films* **2000**, *363*, 152–155.
- 67 Jeong, H.; Zou, D.; Tsutsui, T.; Ha, C.-S. *Thin Solid Films* **2000**, *363*, 279–281.
- 68 Ku, C.-H.; Kuo, C.-H.; Leung, M.-k.; Hsieh, K.-H. *Eur. Polym. J.* **2009**, *45*, 1545–1553.
- 69 Antilla, J. C.; Klapars, A.; Buchwald, S. L. *J. Am. Chem. Soc.* **2002**, *124*, 11684–11688.
- 70 Tsuei, B.; Reddinger, J. L.; Sotzing, G. A.; Soloducho, J.; Katrizky, A. R.; Reynolds, R. *J. Mater. Chem.* **1999**, *9*, 2189–2200.
- 71 Ranger, M.; Rondeau, D.; Leclerc, M. *Macromolecules* **1997**, *30*, 7686–7691.
- 72 Kung, Y.-C.; Hsiao, S.-H. *J. Mater. Chem.* **2011**, *21*, 1746–1754.
- 73 Lee, C.-C.; Wang, P.-S.; Viswanath, M. B.; Leung, M.-k. *Synthesis* **2008**, *9*, 1359–1366.
- 74 Wu, F.-I.; Reddy, D. S.; Shu, C.-F.; Liu, M. S.; Jen, A. K.-Y. *Chem. Mater.* **2003**, *15*, 269–274.
- 75 Grell, M.; Bradley, D. D. C.; Inbaekaran, M.; Woo, E. P. *Adv. Mater.* **1997**, *9*, 798–802.
- 76 Rusalov, M. V.; Druzhinin, S. I.; Uzhinov, B. M. *J. Fluoresc.* **2004**, *14*, 193–202.
- 77 Su, H.-J.; Wu, F.-I.; Tseng, Y.-H.; Shu, C.-F. *Adv. Funct. Mater.* **2005**, *15*, 1209–1216.
- 78 Xia, C.; Advincula, R. C. *Macromolecules* **2001**, *34*, 5854–5859.
- 79 Wu, F.-I.; Dodda, R.; Reddy, D. S.; Shu, C.-F. *J. Mater. Chem.* **2002**, *12*, 2893–2897.